Interplay of subthreshold activity, time-delayed feedback, and noise on neuronal firing patterns

Cristina Masoller, M. C. Torrent, and Jordi García-Ojalvo
Departament de Física i Enginyeria Nuclear, Universitat Politècnica de Catalunya, Colom 11, E-08222 Terrassa, Barcelona, Spain
(Received 12 March 2008; revised manuscript received 23 June 2008; published 8 October 2008)

Feedback connections and noise are ubiquitous features of neuronal networks and affect in a determinant way the patterns of neural activity. Here we study how the subthreshold dynamics of a neuron interacts with time-delayed feedback and noise. We use a Hodgkin-Huxley-type model of a thermoreceptor neuron and assume the feedback to be linear, corresponding effectively to a recurrent electrical connection via gap junctions. This type of feedback can model electrical autapses, which connect the terminal fibers of a neuron's axon with dendrites from the same neuron. Thus the delay in the feedback loop is due basically to the axonal propagation time. We chose model parameters for which the neuron displays, in the absence of feedback and noise, only subthreshold oscillations. These oscillations, however, take the neuron close to the firing threshold, such that small perturbations can drive it above the level for generation of action potentials. The resulting interplay between weak delayed feedback, noise, and the subthreshold intrinsic activity is nontrivial. For negative feedback, depending on the delay, the firing rate can be lower than in the noise-free situation. This is due to the fact that noise inhibits feedback-induced spikes by driving the neuronal oscillations away from the firing threshold. For positive feedback, there are regions of delay values where the noise-induced spikes are inhibited by the feedback; in this case, it is the feedback that drives the neuronal oscillations away from the threshold. Our study contributes to a better understanding of the role of electrical self-connections in the presence of noise and subthreshold activity.

DOI: 10.1103/PhysRevE.78.041907 PACS number(s): 87.19.ll, 87.19.lr, 87.18.Tt, 05.40.Ca

I. INTRODUCTION

Recurrent connections leading to feedback loops are very common in neural tissue, which is characterized by a high density of neuronal cells and connections. A well-known example of recurrent circuit, known to be involved in associative memory recall, is located in the CA3 region of the hippocampus [1,2]. Feedback in neurons can be either excitatory or inhibitory and can arise either from autosynapses or from circuits of connections involving other neurons. These recurrent links require the electrical propagation of action potentials along axons and their chemical transmission through synapses, processes that exhibit a broad spectrum of delay times, ranging from a few milliseconds to tenths of seconds. Since spike frequencies can exceed 10 Hz, delay times can be much longer than the intrinsic characteristic time of the neuron dynamics and cannot be usually neglected.

In fact, time-delayed feedback mechanisms are relevant in many biological systems, including excitable gene regulatory circuits [3], human balance [4], and saccadic eye movements [5]. Within the framework of neuron rate-equation models, a recurrent feedback circuit has been studied by adding to the membrane potential equation a term proportional to the potential at an earlier time [6]. This simplified approach has been successful in the understanding of certain characteristic delay-induced phenomena, such as multistability [7,8] and excitability [9]. In addition, delayed feedback in the FitzHugh-Nagumo paradigmatic model of excitable systems was shown to increase the coherence (measured in terms of the correlation time) and to modulate the main frequencies of the stochastic dynamics in dependence on the feedback delay time [10].

The response of a single neuron to delayed feedback was investigated experimentally by Diez-Martinez and Segundo [11], who studied a pacemaker neuron in the stretch receptor of crayfish. Recurrence was introduced artificially by having each spike trigger electronically a brief stretch after a certain delay. The results showed that with increasing delay the discharge patterns transformed from periodic spikes to trains of spikes separated by silent intervals. Pakdaman *et al.* [12] interpreted this behavior as due to neuronal adaptation mechanisms, which decreased sensitivity along successive firings. By studying models of various levels of complexity (an integrate and fire, a leaky integrator, and a rate-equation model including membrane conductances), with and without adaptation to repeated stimuli, Pakdaman and co-workers found that models including adaptation predicted a dynamics that was similar to that observed experimentally in the crayfish receptor, exhibiting tonic firings for short delays and multiplets or bursts for longer delays.

Delayed feedback provides an additional time scale to the neuronal dynamics. Yet another time scale exists in neurons with subthreshold oscillations [13]. In these neurons, the distance to threshold can be considered to be modulated periodically, which is revealed by a multimodal distribution of interspike intervals [14]. The time delay of the recurrent connections and the period of the subthreshold oscillations can be expected to interact nontrivially. In a previous study [15] we showed that, in the regime of subthreshold oscillations, a weak time-delayed feedback loop can amplify the oscillation amplitude, inducing threshold crossings and firing activity that is organized by the delay. With the aim of providing further insight into the influence of feedback, here we analyze the dynamics using interspike intervals (ISIs) and the firing rate. We also show that feedback-induced activity is robust against the inclusion of noise.

Due to the excitable character of neurons, noise has naturally a large influence on their dynamics, inducing spikes and even increasing their regularity in certain conditions [16].

The influence of noise on a single neuron with a delayed recurrent synaptic connection (but without subthreshold oscillations) was analyzed by Vibert *et al.* [17]. The noise-induced interspike interval distribution was found to change strongly when the delay increased above the natural firing period: for short delays noise irregularizes the firing period, while for long delays the neuron fires with a mean period equal to the delay, as observed without noise.

Some studies also exist on the influence of noise on the firing patterns of neurons with subthreshold oscillations [18], but to our knowledge the joint effect of delayed feedback, noise, and subthreshold activity on neuronal dynamics has not been studied so far. Here we undertake such a study and show that depending on the sign of the delayed feedback, either noise suppresses the delay-induced spikes mentioned above (for inhibitory feedback) or, conversely, delay inhibits noise-induced spikes (for excitatory feedback). In both cases, the phenomenon occurs with the periodicity of the subthreshold oscillations, which underlies the complex interplay between these three different features.

II. MODEL

We use a model displaying sustained subthreshold activity, proposed by Braun *et al.* [19] and developed on the basis of experimental data from shark electroreceptors [20] and mammalian cold receptors [21]. The experimental distributions of interspike intervals in these neuronal types indicate that their activity depends on subthreshold oscillations of the membrane potential. Specifically, those electroreceptors and cold receptors (in their upper temperature range) exhibit an irregular sequence of spikes with a multimodal interspike interval distribution. As mentioned in the Introduction, this multimodality suggests the existence of subthreshold oscillations that operate below but near the spike-triggering threshold. In this situation spikes are triggered by noise, but the subthreshold oscillation period is still reflected in the basic rhythm of the discharge. External stimuli can alter the frequency and/or the amplitude of the oscillations, thus inducing pronounced changes of the neuron firing pattern. In contrast, in the low-temperature range of cold receptors, histograms of interspike intervals do not have a distinct modal structure, but rather seem to reflect pacemaker activity under random fluctuations.

The model proposed by Braun *et al.* produces different types of firing patterns that are also found in cortical neurons [22]. In particular, deterministic firing patterns such as coexistence of spikes and subthreshold oscillations (spikes with skippings), tonic spiking, and bursting patterns have been found as a function of temperature [23]. This rich dynamic behavior is due to the interplay of two sets of de- and repolarizing ionic conductances that are responsible for spike generation and slow-wave potentials [24]. The influence of noise on this model was studied by Feudel *et al.* [25], and model predictions were found to be in good agreement with electrophysiological experiments in the crayfish caudal photoreceptor. Inclusion of a periodic external stimulus leads to a satisfactory reproduction of experiments in paddle-fish, showing that electroreceptor cells contain an intrinsic oscillator that can be synchronized with an external signal [26]. The model has also been used to show the existence of noise-induced synchronization [27] and anticipated synchronization [28]. On the other hand, Sainz-Trapaga *et al.* [29] showed that delayed feedback can increase the amplitude of the subthreshold oscillations beyond threshold, thus leading to feedback-induced spikes. Here we consider the effect of both noise and delayed feedback on this model.

The rate equation for the potential voltage across the membrane, V, is [19]

$$C_M\dot{V} = -I_{Na}(T) - I_K(T) - I_{sd}(T) - I_{sr}(T) - I_l + \eta V(t-\tau) + \xi(t), \tag{1}$$

where C_M is the membrane capacitance, $I_l = g_l(V - V_l)$ is a passive leak current, I_{Na} and I_K are fast sodium and potassium currents, and I_{sd} and I_{sr} are additional slow currents. These four currents are given by

$$I_k = \rho(T) g_k a_k (V - V_k), \tag{2}$$

where k stands for Na, K, sd and sr, g_k are the maximum conductances of the corresponding channels, and the activation variables a_k are given by

$$\frac{da_k}{dt} = \frac{\phi(T)(a_{k\infty} - a_k)}{\tau_k}, \tag{3}$$

for K and sd,

$$\frac{da_{sr}}{dt} = \frac{\phi(T)(-\mu I_{sd} - \theta a_{sr})}{\tau_{sr}}, \tag{4}$$

and $a_{Na} = a_{Na\infty}$. The steady-state activations are defined by

$$a_{k\infty} = \frac{1}{1 + \exp[-s_k(V - V_{0k})]}. \tag{5}$$

The temperature-dependent factors $\rho(T)$ and $\phi(T)$ are

$$\rho(T) = A_1^{(T-T_c)/10}, \quad \phi(T) = A_2^{(T-T_c)/10}. \tag{6}$$

The time-delayed term on the right-hand side of Eq. (1) accounts for the recurrent connection, with η representing the feedback strength and τ the delay time. Here we concentrate on electrical connections mediated by gap junctions, for which the coupling term is linear, while the delay τ represents exclusively the delay associated with axonal propagation prior to the signal recurring onto the neuron. This type of feedback can in principle represent an electrical version of chemical autapses, which are chemical synapses made by a neuron onto itself [30–32]. In our case, the autapses would be *electrical*; i.e., they would be based on gap-junction coupling instead of neurotransmitter exchange and would occur between the terminal fibers at the end of an axon and dendrites from the same neuron. The last term is a Gaussian white noise, with zero mean and correlation $\langle \xi(t)\xi(t') \rangle = 2D\delta(t-t')$, representing the influence of a stochastic environment.

III. RESULTS

The parameters used in the simulations, listed in the caption of Fig. 1 below, are such that in the absence of feedback

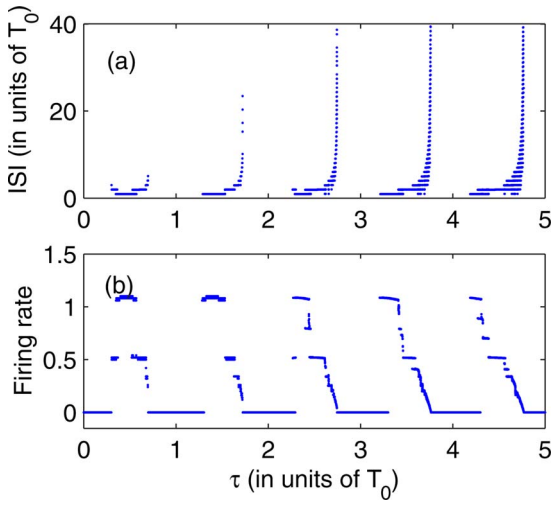

FIG. 1. (Color online) (a) Interspike intervals (normalized to T_0) and (b) firing rate (number of spikes per intrinsic oscillation period) vs the delay time for negative feedback strength, $\eta = -0.001$ mS/cm^2, in the absence of noise. Other parameters are $C_M = 1$ μF/cm^2, $g_l = 0.1$ mS/cm^2, $g_{Na} = 1.5$ mS/cm^2, $g_K = 2$ mS/cm^2, $g_{sd} = 0.25$ mS/cm^2, $g_{sr} = 0.4$ mS/cm^2, $V_l = -60$ mV, $V_{Na} = 50$ mV, $V_K = -90$ mV, $V_{sd} = 50$ mV, $V_{sr} = -90$ mV, $s_{Na} = 0.25$ mV^{-1}, $s_K = 0.25$ mV^{-1}, $s_{sd} = 0.09$ mV^{-1}, $V_{0Na} = -25$ mV, $V_{0K} = -25$ mV, $V_{0sd} = -40$ mV, $\tau_K = 2$ ms, $\tau_{sd} = 10$ ms, $\tau_{sr} = 20$ ms, $\theta = 0.17$, $\mu = 0.012$, $A_1 = 1.3$, $A_2 = 3.0$, and $T_c = 25$ °C.

and noise the neuron displays subthreshold oscillations of period $T_0 \sim 130$ ms. To integrate Eq. (1) in the presence of feedback it is necessary to specify the initial value of the membrane potential V on the time interval $[-\tau, 0]$. Delayed feedback is known to lead to multistability; i.e., different initial conditions lead, after a transient time, to different stable firing patterns [7,8]. Here we chose the initial conditions in such a way that the neuron is oscillating in its natural cycle when the feedback begins to act (i.e., the feedback starts when the neuron is at a random phase of the cycle).

A. Deterministic feedback-induced dynamics

First, we perform numerical simulations of the model equations in the absence of noise. In a previous study [15] we showed that positive feedback decreases the oscillation amplitude, while negative feedback amplifies the oscillations, inducing threshold crossings and firing activity for specific delay values. This is a generic feedback effect, and in order to illustrate the concept with a simple example, in the Appendix we discuss the influence of positive and negative feedback on a limit-cycle oscillator.

Let us first fix $\eta = -0.001$ and vary τ. The numerically calculated ISIs (normalized to the intrinsic subthreshold period T_0) are plotted in Fig. 1(a), and the corresponding firing rate (the average number of firings per intrinsic subthreshold period T_0) is plotted in Fig. 1(b). These figures are done as follows: for each value of τ, after a transient time, we plot all the intervals in between spikes occurring during a time interval NT_0, with N large enough to have good resolution (typically we integrate the model equations for $N = 1500-2000$ subthreshold oscillation periods, after letting transients die away); the firing rate is the averaged rate—i.e., the number of firings divided by N. The firing rate can be slightly larger than 1 because the feedback modifies not only the amplitude, but also the period of the oscillations, and thus for certain delay values there can be more than one firing in a time interval T_0. The feedback-induced modification of the oscillation period was also reported in Ref. [33], which studied the effect of delayed feedback on a noisy oscillator near Andronov-Hopf bifurcation and showed entrainment of the basic period of oscillations to the time delay of the feedback.

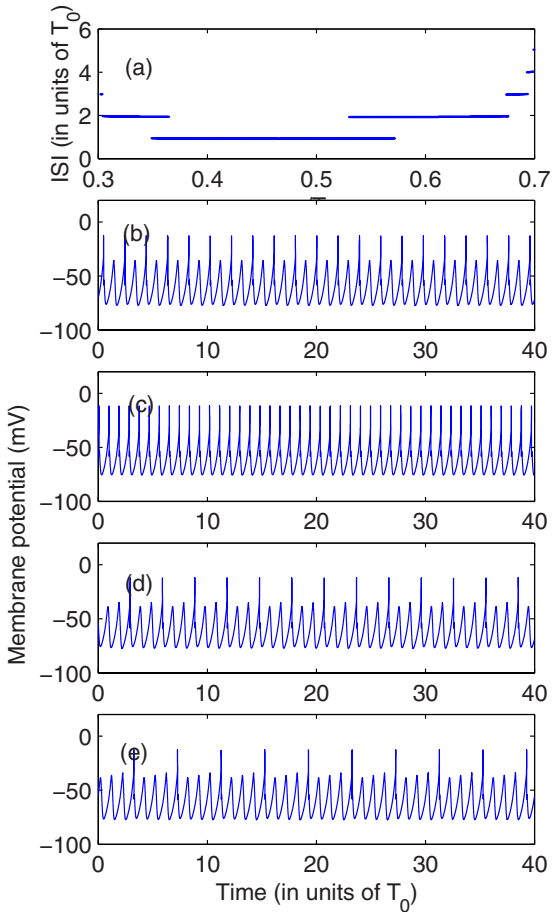

FIG. 2. (Color online) (a) Detail of the ISI profile displayed in Fig. 1(a). Time traces of the membrane potential for $\eta = -0.001$, $\tau/T_0 = 0.31$ (b), 0.5 (c), 0.68 (d), and 0.695 (e).

It can be noticed that the instantaneous feedback is subthreshold; i.e., it does not induce firings; however, the delayed feedback is sub- or suprathreshold, depending on the delay time. The feedback induces firings only in "windows" of the delay time centered at $\tau \sim (n+1/2)T_0$, with n integer. In these windows, the firing pattern is regulated by the value of the delay. Figures 2 and 3 show details in two of these windows (for delays shorter than one subthreshold oscillation period and for delays longer than four periods, respectively). The corresponding firing dynamics is also presented. At the beginning of the first window one can observe spikes with skipping [Fig. 2(b)], which become tonic spikes as τ increases [Fig. 2(c)]. The firings become increasingly sporadic as the delay continues to increase [Figs. 2(d) and 2(e)],

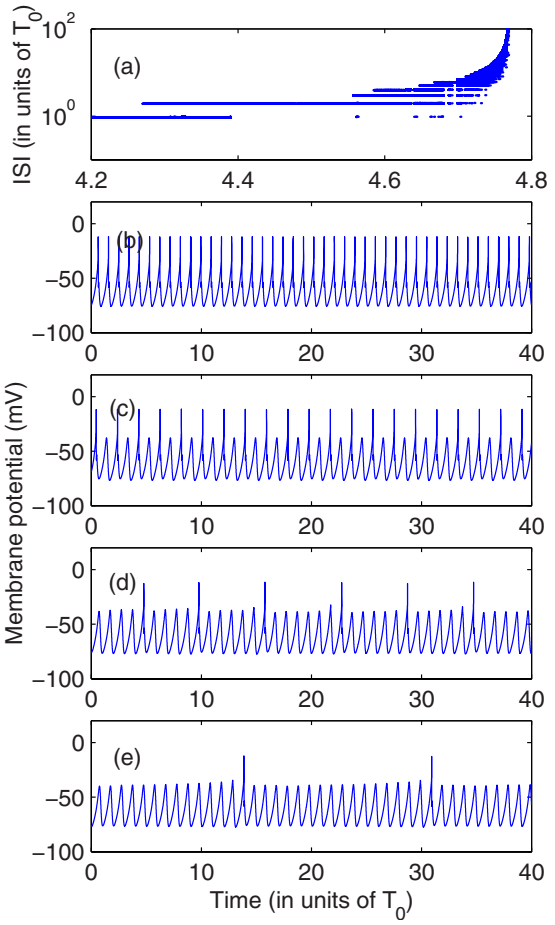

FIG. 3. (Color online) (a) Same as Fig. 2, but for larger delay times. Notice the logarithmic vertical scale. Time traces of the membrane potential for τ/T_0=4.3 (b), 4.5 (c), 4.7 (d), and 4.75 (e).

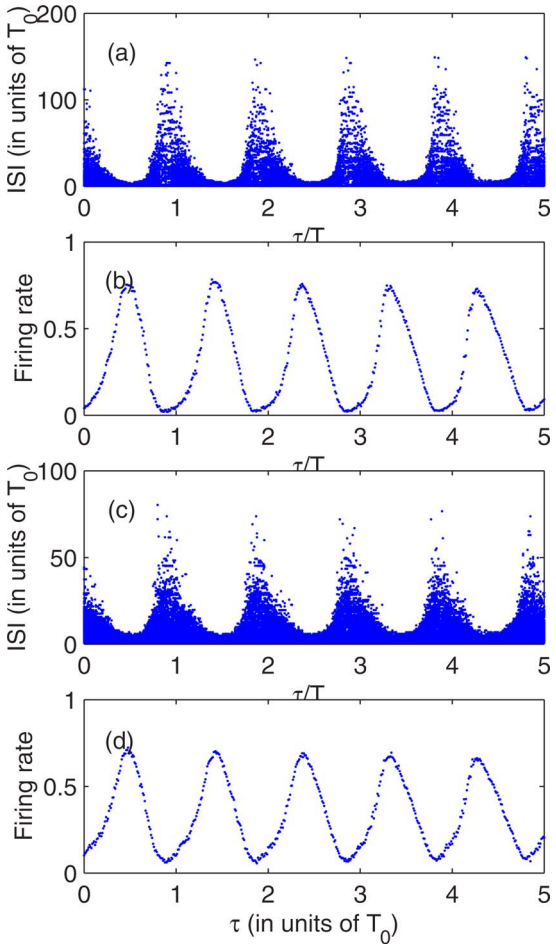

FIG. 4. (Color online) (a),(c) Interspike intervals (normalized to T_0) and (b),(d) firing rate (number of spikes per intrinsic oscillation period) vs the delay time for negative feedback strength, η=−0.001, in the presence of noise: (a), (b) D=0.005 and (c), (d) D=0.01.

until they disappear at the end of the window. A similar behavior is observed for larger delay values (Fig. 3), although in that case the skipping patterns arising in the upper region of the delay window are characterized by a more irregular alternation between the spikes and subthreshold oscillations [see, e.g., Fig. 3(d)], and there is multistability of different firing patterns. The interspike intervals grow sharply to infinity at the end of the short-delay windows—i.e., the spikes disappear abruptly—while there is a smoother transition for longer delays [note the logarithmic vertical scale in Fig. 3(a)].

B. Stochastic dynamics

We now turn to examine the effect of noise in the system. Importantly, in the presence of noise there is a base-line firing rate, depending on the noise intensity, even when the parameters are tuned such that the system is below threshold deterministically, as in the present case. Therefore, in principle one should not expect a situation like the one shown in Fig. 1(b), where for values of the delay time around multiples of the natural period T_0 the system became completely silent; i.e., the firing rate was 0. Figure 4 shows the corresponding plot when noise is included in the simulations, again for negative feedback (the firing rate in the presence of noise is defined in the same way as in the deterministic situation: it is the number of firings per oscillation period, averaged during a time interval NT_0, with N large enough).

It can be observed that the "window" structure reported in the noiseless case (Fig. 1) is robust against noise, although the firing rate does not reach 0 at any delay time [Fig. 4(b)] due to the existence of noise-induced spikes. However, the spikes are more frequent for certain delay times [$\tau \sim (n+1/2)T_0$ with n integer]. Interestingly, we can notice that within some of these delay windows, the firing rate is lower than in the noise-free situation. This is due to the fact that noise can actually inhibit feedback-induced spikes by driving the neuron oscillation away from the firing threshold.

The case of positive feedback is shown in Fig. 5. Remarkably, there are "gap" regions of delay values where the spikes that would be induced by the noise are completely inhibited by the feedback, leading to a vanishing firing rate even in the presence of noise. This happens because the feedback term drives the neuron oscillation away from the threshold. These silent "gaps" shrink and eventually vanish as the noise strength is increased.

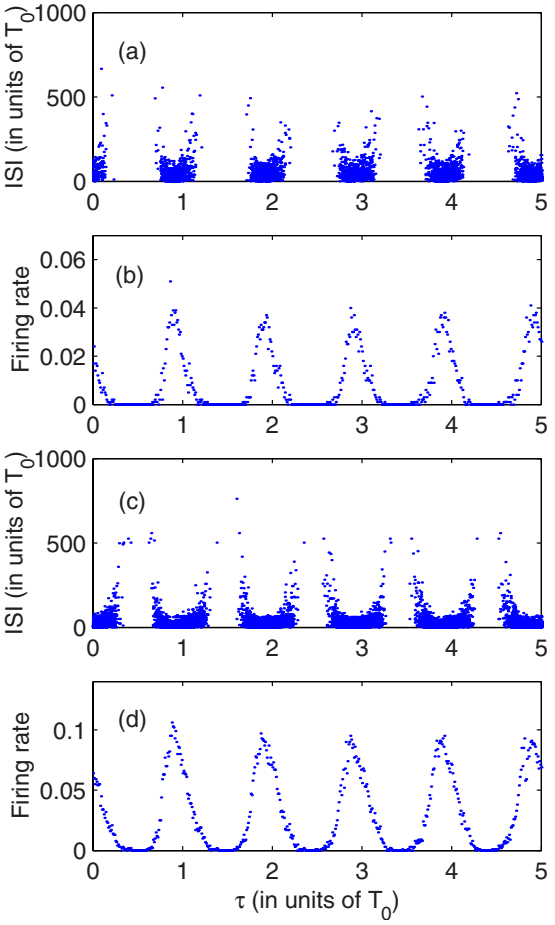

FIG. 5. (Color online) (a),(c) Interspike intervals (normalized to T_0) and (b),(d) firing rate (number of spikes per intrinsic oscillation period) vs the delay time for positive feedback strength, $\eta=0.001$, in the presence of noise: (a), (b) $D=0.005$ and (c), (d) $D=0.01$.

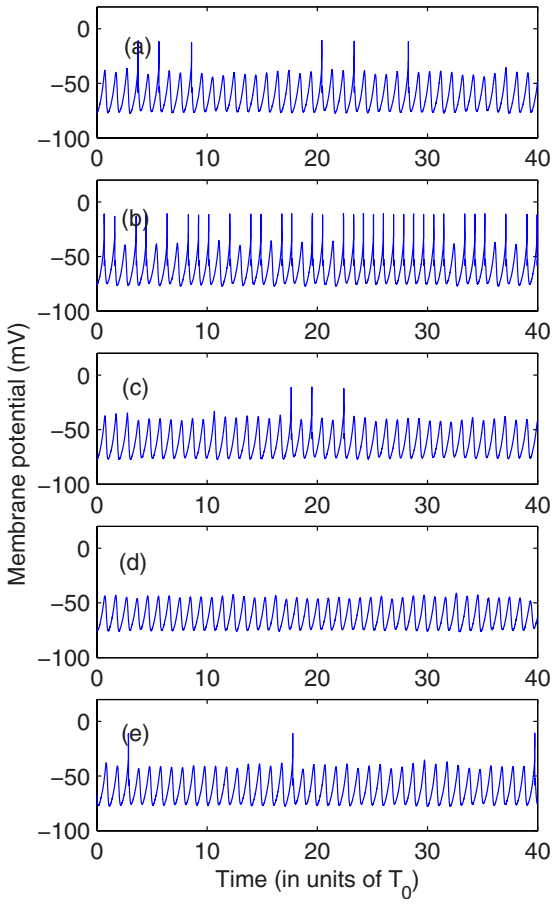

FIG. 6. (Color online) Membrane potential when noise is included in the simulations ($D=0.01$). No feedback (a), negative feedback ($\eta=-0.001$) (b),(c), and positive feedback ($\eta=0.001$) (d),(e). The delay time is $\tau=T_0/2$ (b),(d) and $\tau=T_0$ (c),(e).

A few examples of time traces of the membrane potential are displayed in Fig. 6. In Fig. 6(a) there is no feedback and the firings are only noise induced; in Figs. 6(b) and 6(c), there is negative feedback and two different delay times, one such that, without noise, there are periodic spikes [$\tau=T_0/2$; the noiseless spike pattern is presented in Fig. 2(c)]. With the inclusion of noise, it can be seen in Fig. 6(b) that some spikes are skipped. The other delay $\tau=T_0$ is such that the firing rate is about the same as for instantaneous feedback [see Fig. 4(d)]. Figures 6(d) and 6(e) display time traces of the membrane potential when positive feedback is included, and again two delay times are considered, one such that the delayed feedback inhibits noise-induced spikes [Fig. 6(d)] and the other such that the firing rate is about the same as for instantaneous feedback [Fig. 6(e)].

Finally, to gain insight into (i) how positive feedback interferes with stochastically generated spikes and (ii) how noise interferes with deterministically feedback-induced spikes we analyzed the probability density function of ISIs. We found that both η and τ have complex effects on the ISI distribution. Several distributions are presented in Figs. 7 and 8. Figure 7(a) displays the distribution in the absence of feedback. A multipeaked distribution is observed, which can be interpreted in the same way as in Ref. [34] for resonant neurons: if a spike occurs at time $t=0$, the probability of another spike occurring at a latter time t is modulated by the subthreshold oscillation. Figures 7(b) and 7(c) display the effect of positive feedback. We observe that it enlarges the tail of the distribution and there is a delay-dependent modification of the distribution shape.

Next we consider the influence of noise on feedback-induced irregularly timed spikes. The ISI distribution in the absence of noise is presented in Fig. 8(a), and the effect of noise is displayed in Figs. 8(b) and 8(c). Noise tends to broaden the distribution and also modifies its shape, with a dip appearing at the value of the delay time ($\tau=4.7T_0$).

The influence of feedback and noise on a bistable system was studied in Ref. [35]. It was shown that the feedback modifies the shape of the distribution of residence times (the time spent in a well before jumping to the other), increasing or decreasing the probability of residence times shorter than the delay time, depending on the sign of the feedback. This effect was understood in terms of a simple two-state model with transition rates depending on the earlier state of the system. More recently, for a linear oscillator driven by colored Gaussian noise, modeling a resonant neuron, the probability density of the first passage time [the time after which $x(t)$ reaches certain level for the first time] was calculated based on a non-Markovian approximation [37], and complex

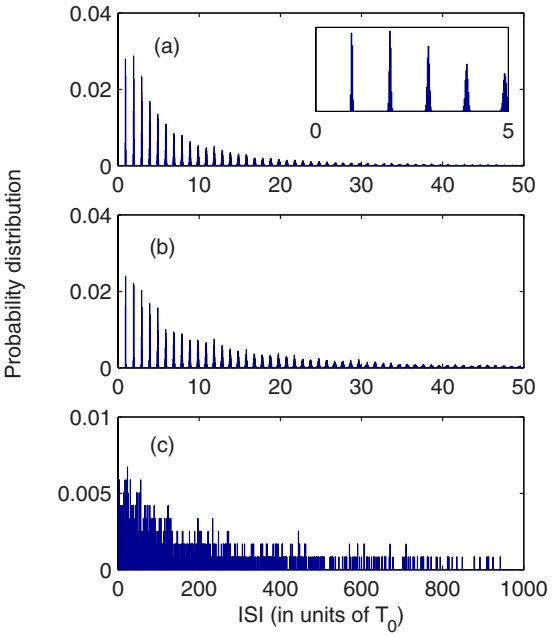

FIG. 7. (Color online) Probability density function of interspike intervals for fixed noise (D=0.01) and varying feedback. (a) Without feedback, (b),(c) with positive feedback [η=0.0001 in (b), η =0.0005 in (c)] and a delay value such that the feedback decreases the firing rate ($\tau=T_0/2$). In (a) the inset displays in detail the first five peaks of the distribution.

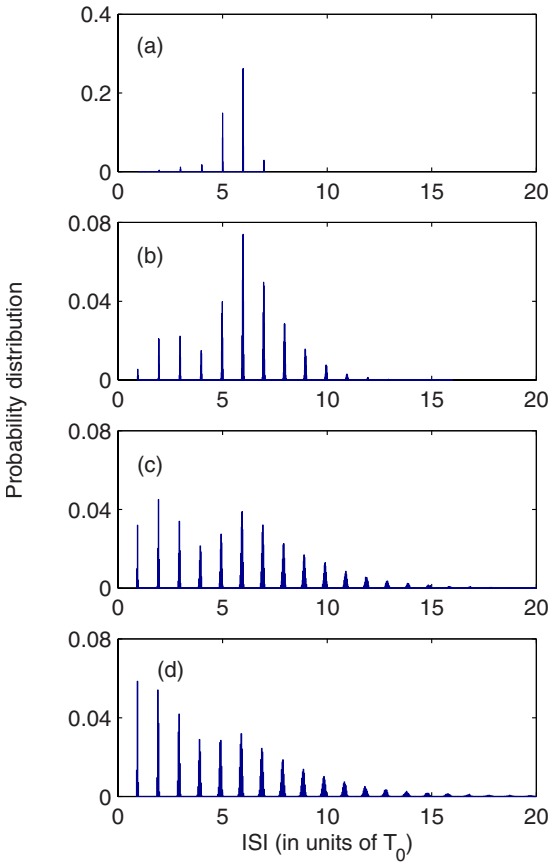

FIG. 8. (Color online) Probability density function of interspike intervals for fixed negative feedback (η=−0.001) and varying noise. The delay value is such that there is an irregular alternation of spikes and subthreshold oscillations [$\tau=4.7T_0$; a spike train is shown in Fig. 3(d)]. Without noise (a) and D=0.001 (b), 0.005 (c), and 0.01 (d).

structures, characteristics of underdamped dynamics, were revealed. The interpretation of the effects of delayed feedback on the ISI distribution, based on these previous studies, and their relation with common noise effects in excitable systems [36], such as stochastic and coherence resonance, resonant activation, etc., is the subject of ongoing work.

IV. SUMMARY AND CONCLUSIONS

We studied the dynamics of a neuron with subthreshold oscillations under the influence of delayed feedback and noise. We simulated numerically a Hodgkin-Huxley-type model, extended to account for a feedback circuit with an additional time-delayed linear term in the membrane voltage equation. The feedback term is assumed linear, corresponding effectively to an electrical connection via gap junctions. This type of feedback can model the electrical analog of chemical autapses, which would connect linearly the terminal fibers of a neuron's axon to its own dendrites. Thus, the delay time is due basically to axonal propagation along the feedback loop. The model parameters are such that the neuron displays only subthreshold oscillations in the absence of feedback and noise. The neuronal oscillations are near the firing threshold, and small perturbations can drive the oscillations above the level for generation of action potentials. In this situation we find a complex interplay of weak delayed feedback and noise with the subthreshold intrinsic activity.

For negative feedback, the oscillation amplitude is enhanced, and this enhancement is more pronounced for certain delay values. In the noise-free situation, this leads to the existence of specific "windows" of delay values where feedback-induced spikes occur. When noise is included in the simulations, firings are observed for all delay values, but for certain delays, the firing rate can be lower than in the noise-free situation. This is due to the fact that the noise can inhibit some of the feedback-induced spikes by randomly driving the neuron oscillations away from the firing threshold.

For positive feedback, in the noise-free situation there are no firings because the feedback reduces the oscillation amplitude. However, this reduction is more pronounced for certain delays, and when noise is included in the simulations, there are "gap regions" of delay values where the noise-induced spikes are inhibited by the feedback; in this case, it is the feedback that drives the neuron oscillations away from the threshold.

Taken together, our results show that subthreshold activity nontrivially modulates the response of a neuron to delayed feedback and noise.

Our study aims to contribute to a better understanding of the role of electrical autapses, in the presence of noise and subthreshold oscillations. While their functional significance is not yet clear, chemical autapses have been recently suggested to have important roles in regulating spike timing [38], since a blockade of autaptic transmission resulted in

degraded spike temporal precision. Our results shed light on the interplay of electrical "autaptic" delayed feedback and noise, when the neuron displays intrinsic subthreshold oscillations. It would be of interest to extend this study to consider the case of chemical synaptic coupling, where delays due to neurotransmitter release and binding would be even more evident. It would also be interesting to extend this study to spiking neurons that display, in the absence of feedback or noise, deterministic spike patterns, such as tonic spikes or bursting.

ACKNOWLEDGMENTS

C.M. is supported by the "Ramon y Cajal" program (Spain). Financial support was also provided by the European Commission (GABA Project No. FP6-NEST 043309), the Ministerio de Educación y Ciencia (Spain, project ORDEN), and the Generalitat de Catalunya (Spain, project 2005SGR-00457). J.G.O. acknowledges support from Instituto de Salud Carloss III (Spain, Project No. RD06/0060/0017).

APPENDIX

To explain the influence of feedback on the amplitude and on the frequency of the subthreshold oscillations, here we consider a simple model, consisting of a limit-cycle oscillator. In the literature, several authors have studied the influence of linear and nonlinear delayed feedback on a limit-cycle oscillator (see, e.g., [32,39,40] and references therein). Feedback-induced phenomena such as multistability, phase slips, chaos, and excitability are well known. Here we limit ourselves to consider the influence of feedback when it is a *small* perturbation to the oscillator and show how, depending on the sign of the feedback and its delay time, the amplitude and the frequency of the oscillator are modified. The rate equation for a limit-cycle oscillator is

$$\dot{z} = (1 + i\omega_0 - |z|^2)z + \eta z(t - \tau), \tag{A1}$$

where z is a complex variable, η is the feedback coefficient, which is assumed real, and τ is the delay time.

In the absence of feedback the amplitude of the limit cycle is $A_0=1$ and its frequency is ω_0 (the natural oscillation period being $T_0=2\pi/\omega_0$). In the presence of feedback, both the amplitude A and the frequency ω change with η and τ, as displayed in Fig. 7. For $\eta>0$ the amplitude [Fig. 9(a)] exhibits local minima at $\tau=(n+1/2)T_0$ with $n=0,1,\ldots$. For $\eta<0$ local maxima are the ones located at $\tau=(n+1/2)T_0$ with $n=0,1,\ldots$, Fig. 9(c). For τ larger than one or two natural periods periods, the frequency varies with τ in a piecewise linear way, exhibiting discontinuous jumps at $\tau=(n+1/2)T_0$ for positive feedback, Fig. 9(b), and at $\tau=nT_0$ for negative feedback, Fig. 9(d). A similar entrainment of the basic period of oscillations by time delay was reported in Ref. [33], which studied the effect of delayed feedback on noise-induced motion in a self-oscillator near an Andronov-Hopf bifurcation and in a threshold system.

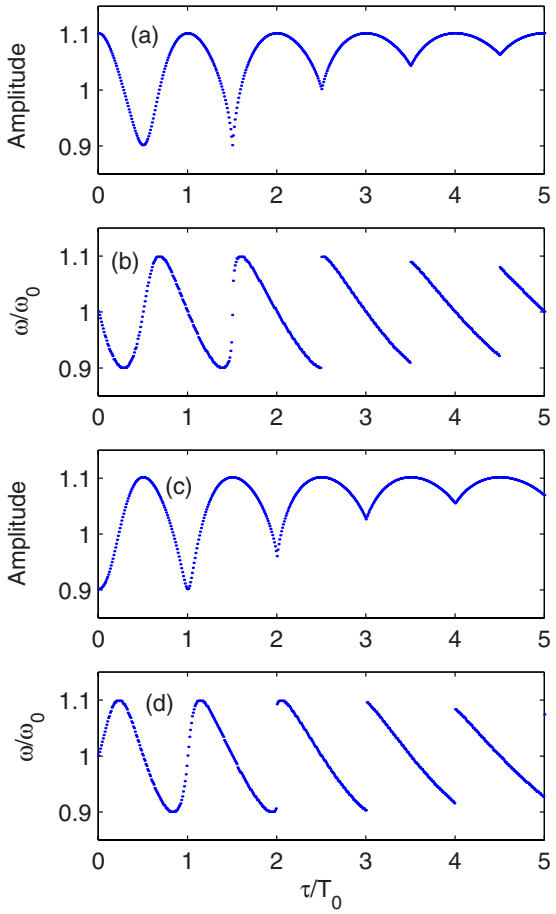

FIG. 9. (Color online) Amplitude (a),(c) and frequency (c),(d) of the limit-cycle oscillator, Eq. (A1), with positive feedback, $\eta=0.1$ (a),(b) and with negative feedback, $\eta=-0.1$ (c),(d). $\omega_0=1$.

The influence of feedback on the neuronal model considered here is expected to be more complex, because the feedback acts only on one variable (the membrane potential) and the model has additional variables, the conductance currents, that present different relaxation time scales (there are two fast and two slow currents). Nevertheless, it can be seen in Fig. 1 that for negative feedback spikes occur in windows centered at $\tau=(n+1/2)T_0$, and this agrees with the limit-cycle model since for those values the amplitude of the limit cycle exhibits local maxima. For positive feedback, in Fig. 5 it can be observed that noise-induced firings are suppressed in windows centered at $\tau=(n+1/2)T_0$, and this agrees qualitatively with the limit-cycle model, since for those delay values, the oscillation amplitude is minimum. An important difference should be noticed, and it is that in the limit cycle the effects of positive and negative feedback are symmetric (see Fig. 9), but they are not symmetric in the neuron model, where negative feedback increases the oscillation amplitude, while positive feedback decreases the oscillation amplitude, for all τ. We speculate that this difference arises because in the neuron model there is feedback only in the rate equation for the membrane potential.

[1] D. Debanne, B. H. Gahwiler, and S. M. Thompson, J. Physiol. (London) **507**, 237 (1998).
[2] K. Nakazawa, M. C. Quirk, R. A. Chitwood *et al.*, Science **297**, 211 (2002).
[3] G. M. Süel, J. Garcia-Ojalvo, L. M. Liberman, and M. B. Elowitz, Nature (London) **440**, 545 (2006).
[4] J. L. Cabrera and J. G. Milton, Phys. Rev. Lett. **89**, 158702 (2002).
[5] K. Mergenthaler and R. Engbert, Phys. Rev. Lett. **98**, 138104 (2007).
[6] R. E. Plant, SIAM J. Appl. Math. **40**, 150 (1981).
[7] J. Foss, A. Longtin, B. Mensour, and J. Milton, Phys. Rev. Lett. **76**, 708 (1996).
[8] J. Foss and J. Milton, J. Neurophysiol. **84**, 975 (2000).
[9] T. Piwonski, J. Houlihan, T. Busch, and G. Huyet, Phys. Rev. Lett. **95**, 040601 (2005).
[10] T. Prager, H. P. Lerch, L. Schimansky-Geier, and E. Schöll, J. Phys. A **40**, 11045 (2007).
[11] O. Diez-Martinez and J. P. Segundo, Biol. Cybern. **47**, 33 (1983).
[12] K. Pakdaman, J. F. Vibert, E. Bousssard, and N. Azmy, Neural Networks **9**, 797 (1996).
[13] A. Alonso and R. Llinás, Nature (London) **342**, 175 (1989).
[14] J.-L. Xing, S.-J. Hu, and K.-P. Long, Brain Res. **901**, 128 (2001).
[15] C. Masoller, M. C. Torrent, and García-Ojalvo, Lect. Notes Comput. Sci. **4668**, 963 (2007).
[16] B. Lindner, J. García-Ojalvo, A. Neiman, and L. Schimansky-Geier, Phys. Rep. **392**, 321 (2004).
[17] J. F. Vibert, F. Alvarez, and J. Pham, BioSystems **48**, 255 (1998).
[18] M. T. Huber and H. A. Braun, BioSystems **89**, 38 (2007).
[19] H. A. Braun, M. T. Huber, M. Dewald, K. Schafer, and K. Voigt, Int. J. Bifurcation Chaos Appl. Sci. Eng. **8**, 881 (1998).
[20] H. A. Braun, H. Wissing, K. Schafer, and M. C. Hirsch, Nature (London) **367**, 270 (1994).
[21] H. A. Braun, H. Bade, and H. Hensel, Pfluegers Arch. **386**, 1 (1980).
[22] H. A. Braun, K. Voigt, and M. T. Huber, BioSystems **71**, 39 (2003).
[23] W. Braun, B. Eckhardt, H. A. Braun, and H. Huber, Phys. Rev. E **62**, 6352 (2000).
[24] H. A. Braun, M. T. Huber, N. Anthes, K. Voigt, A. Neiman, X. Pei, and F. Moss, Neurocomputing **32**, 51 (2000).
[25] U. Feudel, A. Neiman, X. Pei, W. Wojtenek, H. Braun, M. Huber, and F. Moss, Chaos **10**, 231 (2000).
[26] A. Neiman, X. Pei, D. Russell, W. Wojtenek, L. Wilkens, F. Moss, H. A. Braun, M. T. Huber, and K. Voigt, Phys. Rev. Lett. **82**, 660 (1999).
[27] C. S. Zhou and J. Kurths, Chaos **13**, 401 (2003).
[28] M. Ciszak, O. Calvo, C. Masoller, C. R. Mirasso, and R. Toral, Phys. Rev. Lett. **90**, 204102 (2003).
[29] M. Sainz-Trapaga, C. Masoller, H. A. Braun, and M. T. Huber, Phys. Rev. E **70**, 031904 (2004).
[30] G. Tamas, E. H. Buhl, and P. Somogyi, J. Neurosci. **17**, 6352 (1997).
[31] C. S. Herrmann and A. Klaus, Int. J. Bifurcation Chaos Appl. Sci. Eng. **14**, 623 (2004).
[32] G. C. Sethia and A. Sen, Phys. Lett. A **359**, 285 (2006).
[33] A. G. Balanov, N. B. Janson, and E. Schöll, Physica D **199**, 1 (2004).
[34] T. Verechtchaguina, L. Schimansky-Geier, and I. M. Sokolov, Phys. Rev. E **70**, 031916 (2004).
[35] C. Masoller, Phys. Rev. Lett. **90**, 020601 (2003).
[36] B. Lindner, J. Garcia-Ojalvo, A. Neiman, and L. Schimansky-Geier, Phys. Rep. **392**, 321 (2004).
[37] T. Verechtchaguina, I. M. Sokolov, and L. Schimansky-Geier, Europhys. Lett. **73**, 691 (2006).
[38] A. Bacci and J. R. Huguenard, Neuron **49**, 119 (2006).
[39] D. V. Ramana Reddy, A. Sen, and G. L. Johnston, Physica D **144**, 335 (2000).
[40] G. C. Sethia, J. Kurths, and A. Sen, Phys. Lett. A **364**, 227 (2007).